Microwave Dielectric Measurements of Erythrocyte Suspensions

Jian-Zhong Bao,* Christopher C. Davis,* and Mays L. Swicord‡
*Department of Electrical Engineering, University of Maryland, College Park, Maryland 20742, and ‡Center for Devices and Radiological Health, Food and Drug Administration, Rockville, Maryland 20857 USA

ABSTRACT Complex dielectric constants of human erythrocyte suspensions over a frequency range from 45 MHz to 26.5 GHz and a temperature range from 5 to 40°C have been determined with the open-ended coaxial probe technique using an automated vector network analyzer (HP 8510). The spectra show two separate major dispersions (β and γ) and a much smaller dispersion between them. The two major dispersions are analyzed with a dispersion equation containing two Cole-Cole functions by means of a complex nonlinear least squares technique. The parameters of the equation at different temperatures have been determined. The low frequency behavior of the spectra suggests that the dielectric constant of the cell membrane increases when the temperature is above 35°C. The real part of the dielectric constant at ~3.4 GHz remains almost constant when the temperature changes. The dispersion shifts with temperature in the manner of a thermally activated process, and the thermal activation enthalpies for the β- and γ-dispersions are 9.87 ± 0.42 kcal/mol and 4.80 ± 0.06 kcal/mol, respectively.

INTRODUCTION

Dielectric measurements made over a wide frequency range provide one of the most reliable means for obtaining structural and dynamic information about materials. Low frequency measurements of this kind have been widely made; however, dielectric properties in the GHz range have been less studied. During the last 10 years, the open-ended coaxial probe technique with an automated vector network analyzer has been fairly extensively applied to liquids, colloids, and suspensions, because it is much more convenient to use than transmission line methods (Baker-Jarvis et al., 1990), especially for small quantities of liquid. It covers a much wider frequency range and provides many more frequency points than resonant cavity methods, although the latter are in general more accurate (Dube, 1988). Dielectric information about living cells is of importance for a fundamental understanding of the interaction between electromagnetic fields and biological systems (Edwards et al., 1992; Schwan, 1985; Pethig, 1984) and for clinical applications (Chou, 1992; Foster and Cheever, 1992). Among living cells, erythrocytes have been widely studied with a variety of experimental techniques (Bone et al., 1993; Ballario et al., 1984). However, most of these studies are in the radio frequency range, and there are few systematic studies of the temperature dependence of dielectric properties of living cells above 5 GHz (Michaelson and Lin, 1987; Schwan and Foster, 1980). The dielectric behavior of such systems is mainly due to the dynamic response of their constituents to the external field and should be a reflection of their dominant physiological and physical processes. This has been a subject of both experimental and theoretical study for many years (Asami et al., 1988; Schwan, 1957). In this paper, as a continuation of our previous low-frequency (1 Hz to 10 MHz) studies on human erythrocytes (Bao et al., 1992, 1993), we report the microwave dielectric spectra of human erythrocyte suspensions and their complex nonlinear analysis in the frequency range from 45 MHz to 26.5 GHz and for temperatures from 5 to 40°C. At each temperature, the measurements show two separate major dispersions, which are commonly referred as the β- and γ-dispersions. The β-dispersion, centered in the radio frequency range, is largely due to the occurrence of Maxwell-Wagner effects at the interface between the cell membrane and the aqueous phase. Charging and relaxation processes on the cell membrane, involving conducting ions within and outside the cell, are related to the properties of the cell membrane, the cytoplasm, and the extracellular medium, such that a study of the β-dispersion can provide information about cell membrane and cytoplasm. The γ-dispersion, centered in the microwave frequency range, is attributed to the relaxation of water molecules in the bulk phase. Apart from the two dispersions mentioned above, a much smaller dispersion centered around 1 GHz has also been observed. It has been suggested that this small dispersion results from the relaxation of bound water and perhaps side chain motions of macromolecules (Steinhoff et al., 1993; Pethig, 1984). The conformation and the thermodynamic properties of these macromolecules strongly affect the water molecules around them, and consequently this small dispersion. Our understanding of it in terms of mechanisms is incomplete.

Received for publication 17 September 1993 and in final form 23 March 1994.

Address reprint requests to Christopher C. Davis, Department of Electrical Engineering, University of Maryland, College Park, MD 20742. Tel.: 301-405-3637; Fax: 301-314-9281; E-mail: davis@eng.umd.edu.

0006-3495/94/06/2173/08 $2.00

EXPERIMENTAL PROCEDURES

A block diagram of our HP 8510 network analyzer and measurement configuration is shown in Fig. 1. One end of a right-angle semi-rigid coaxial

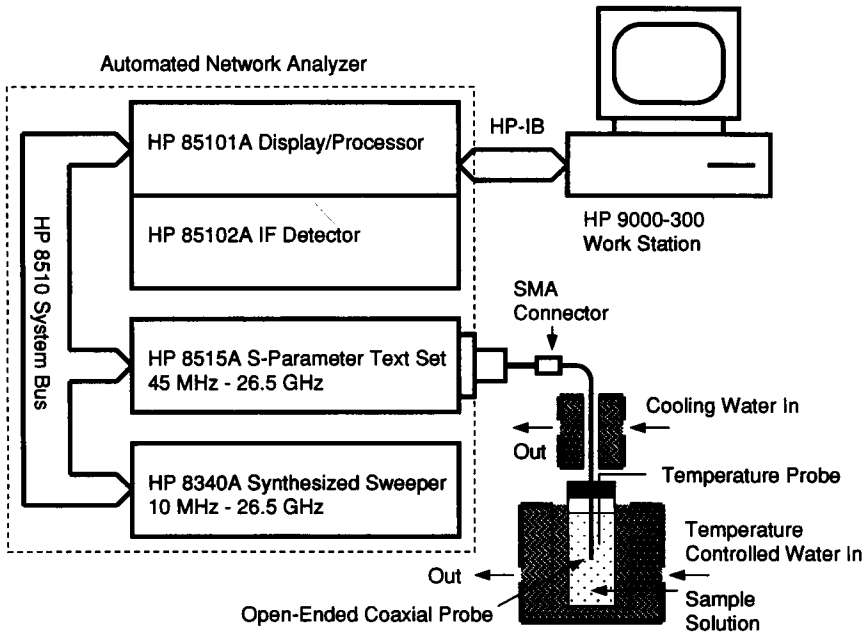

FIGURE 1 Block diagram of HP 8510A vector network analyzer and measurement system.

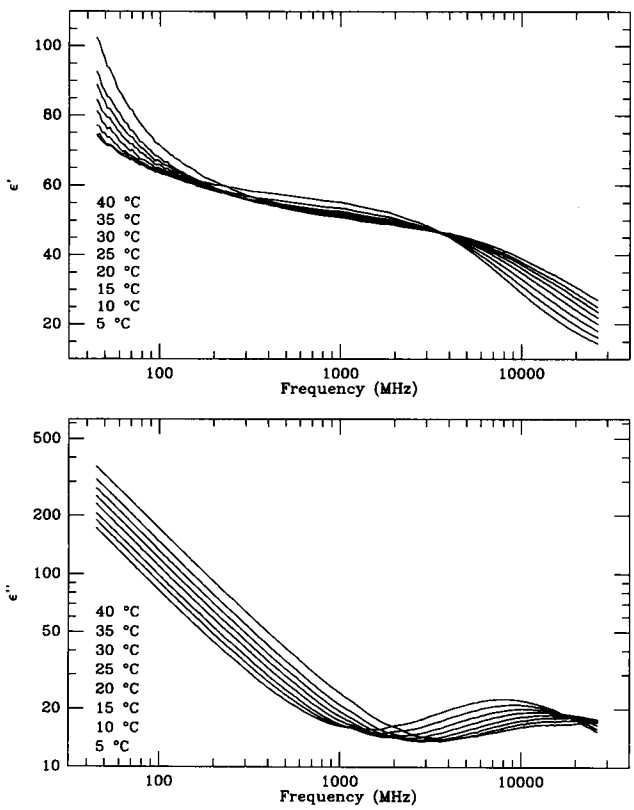

FIGURE 2 Dielectric spectra of human erythrocyte suspensions for selected temperatures from 5 to 40°C with equal 5°C increments.

transmission line was connected to one test port of the S-parameter test set (HP 8515A) through a SMA connector, while the other was dipped into the sample solution. The synthesized sweeper (HP 8340A) was set in the cw mode, and was controlled by a work station (HP 9000–300) such that the whole frequency range was swept on a logarithmic scale over 201 frequency points. Each sweep takes less than 1 min. A complex impedance Z that depends on the dielectric properties of the sample was determined from the complex reflection coefficient (Γ) at the interface between the flat end of the probe and the sample, where

$$Z = Z_0 \frac{1 + \Gamma}{1 - \Gamma'}, \tag{1}$$

and Z_0 is the characteristic impedance of the coaxial line. In a first order approximation, the interface between tip and sample can be modeled as two parallel capacitors (Athey et al., 1982; Stuchly et al., 1982), which gives an impedance

$$Z = \frac{1}{j\omega(C_f + \epsilon C_o)}, \tag{2}$$

where C_f is a capacitance determined by fringing-fields effects inside the probe, C_o is a capacitance that depends on effects of the fringing-fields outside the probe tip that couple to the sample, $j = \sqrt{-1}$, ω is the angular frequency, and $\epsilon = \epsilon' - j\epsilon''$ is the complex dielectric constant of the sample. From Eqs. 2 and 3 we can find ϵ from Γ. However, Γ is not the actual measured reflection coefficient (ρ_m) from the network analyzer, since the latter includes not only information from the interface but also error effects from the coaxial line, connectors, and container. To eliminate these systematic errors, a calibration procedure, which is based on a linear assumption and involves three standard measurements and some mathematical manipulation of a scattering matrix, was used. A simple matrix derivation gives (see Appendix):

$$\epsilon = \frac{A_1\rho_m - A_2}{A_3 - \rho_m}, \tag{3}$$

where A_1, A_2, and A_3 are three frequency-dependent complex constants, related to the elements of the scattering matrix, and furthermore, A_1 and A_2 are also related to Z_0, C_f, and C_o. The three constants can be determined by three standard measurements at each frequency point. The three standards are an "open," which gives $\epsilon = 1$, a short, which gives $\Gamma = -1$, and a known solution, which in this case is the saline we use to prepare the sample. The "open" is easily obtained by exposing the open end to the air. The short circuit can be achieved by gently pressing a piece of aluminum foil against the open end. To get good electrical contact, the end should be flat and any oxidation layer should be polished off carefully. When a good short is achieved, ρ_m, shown on the display of the HP 8510, shows a stable 180° phase shift with respect to the open measurements at low frequencies, while its magnitude remains unchanged. A standard liquid measurement was obtained by dipping the probe into the solution. An analytical equation was utilized to give the complex dielectric permittivity for saline at different temperatures and molarities. The analytical equation given by Stogryn

(1971), which has been widely used, contains errors so we use our own version of equations for the complex dielectric constant of saline based on a re-evaluation of earlier data (Weyl, 1964; Malmberg and Maryott, 1956).

The probe is 2.2 mm in diameter and about 15 cm in length, and was preconditioned three times in the temperature range from −4 to 85°C to decrease the possible deformation of the Teflon in the probe (Colpitts, 1993). The deformation of Teflon in the coaxial line will become smaller and smaller during the temperature cycling because of the friction between the conductors and the dielectric. After the above treatment, geometrical deformation of the probe caused by changing temperature becomes negligibly

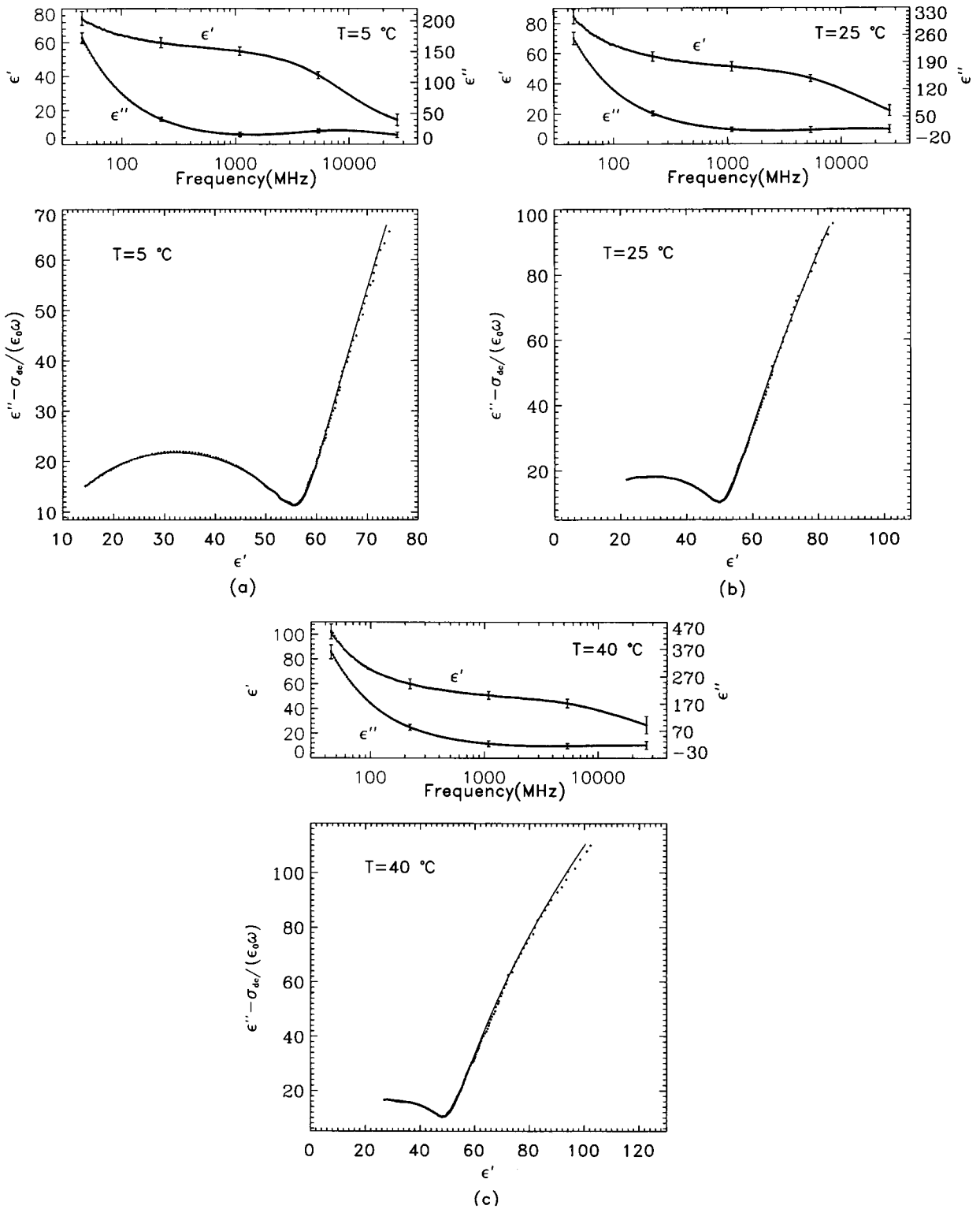

FIGURE 3 Comparison between the CNLS fits (*solid lines*) and the experimental data (●) for 5°C (*a*), 25°C (*b*), and 40°C (*c*). The contribution of σ_{dc}, which is determined from CNLS fits, has been subtracted in the Cole-Cole plots, where only a small high-frequency portion of the arc for the β-dispersion is shown.

small in the temperature range of this experiment, which is much smaller than the range of temperature cycling. To further minimize systematic errors caused by using the probe at different temperatures, we applied appropriate calibration files that were obtained from standard saline at corresponding temperatures to calibrate the measurements at each temperature. In this way, we take any remaining small deformations, if there are such, into account.

Approximately 20 ml of human erythrocytes was drawn by venous puncture and mixed with saline (0.154 M). Sample cells are sedimented by centrifugation at about 3500 × g for about 30 min, and the plasma and buffy coat above the erythrocytes are removed. This process was repeated twice to ensure purity of the erythrocyte sample. About 5 ml of packed cells were used for the measurements. To achieve good quality data, the relative position of the probe in the container should be kept the same through all the liquid measurements. This is particularly important when the quantity of sample is small and to minimize a resonant feature observed around 2 GHz, which is essentially due to the finite volume of sample. Care must be taken to make sure that there are no air bubbles in the sample, especially near the flat end of the probe. The sample solution in its container is in intimate thermal contact with a water-jacketed brass enclosure whose temperature is controlled by a high speed constant temperature circulator (Neslab RTE-110D).

RESULTS AND DISCUSSION

Fig. 2 presents the experimental results in the temperature range from 5 to 40°C for equal 5°C increments: each of these spectra show two major dispersions, which are commonly referred as the β- and γ-dispersions, although only the high-frequency tail of the β-dispersion is covered in this frequency range. Between the two major dispersions there is a much smaller dispersion. At frequencies above 300 MHz, cell membranes pose no hindrance to the passage of electrical current, and their dielectric properties are dominated by water and proteins. There are three important features in the spectra: 1) The low-frequency portion of both ϵ' and ϵ'', in the β-dispersion region, shows a larger jump from 35 to 40°C than the series jumps in the same temperature intervals at lower temperatures, which is consistent with the phase transition temperature we found previously (Bao et al., 1992). 2) ϵ' between 0.5 and 2 GHz shows a stronger temperature dependence at lower temperature and decreases while temperature increases. 3) At ~3.4 GHz, the value of ϵ' is almost a constant with temperature, which is essentially due to water molecules. ϵ' increases with temperature when frequency is above this value while it decreases with temperature for frequencies lower than but not far away from this point. The shape and temperature dependence of the broad symmetric peaks of ϵ'' in the GHz range suggest that the resonant absorption of microwave energy is due to water dipoles, which implies that non-thermal processes are insignificant compared to thermal effects, at least at the single cell level. To analyze the β- and γ-dispersions, we have found that they can be represented well by two Cole-Cole functions:

$$\epsilon_{cc} = \epsilon_h + \sum_{m=1,2} \frac{\Delta\epsilon_m}{1 + (j\omega\tau_m)^{\alpha_m}} + \frac{\sigma_{dc}}{j\omega\epsilon_0}, \qquad (4)$$

where ϵ_h is the high-frequency limit of the dielectric constant, $\Delta\epsilon_m$ is the dielectric decrement of the dispersion, τ_m is a relaxation time, $0 < \alpha_m < 1$, σ_{dc} is the dc conductivity, and ϵ_0 is the dielectric constant of the vacuum. The small dispersion between the two major dispersions has not been taken into account because 1) it has a much smaller magnitude than the other two dispersions; 2) a large portion of it was overlaid with other dispersions; and 3) introducing additional parameters in fitting would not be sound statistically.

The Cole-Cole function is only an empirical representation, which gives a power-law relation between permittivity and frequency, and has been widely used in dielectric analysis (Macdonald, 1987; Bottcher and Bordewijk, 1978). Many types of systems, especially disordered systems, display such non-Debye behavior (Grochulski et al., 1992; Ngai, 1987), which is usually ascribed to the presence of a distribution, possibly of a fractal nature (Schroeder, 1991; Dissado, 1990; Niklasson, 1987), of some physical quantity in space, time, or energy. Although there exist quite a few ideas yielding these power-law relations (Zhou and Bagchi, 1992; Nee and Zwanzig, 1970), there is no universally accepted theory for them. The exponent α_m is a measure of deviation from a simple Debye relation and can be taken mathematically as an indicator of the distribution width of time constants symmetrically centered at τ_m. A smaller α_m implies a broader distribution range, and $\alpha_m = 1$ gives a single time constant relaxation process (Debye behavior). An accepted physical explanation of a distribution of time constants is that different relaxation

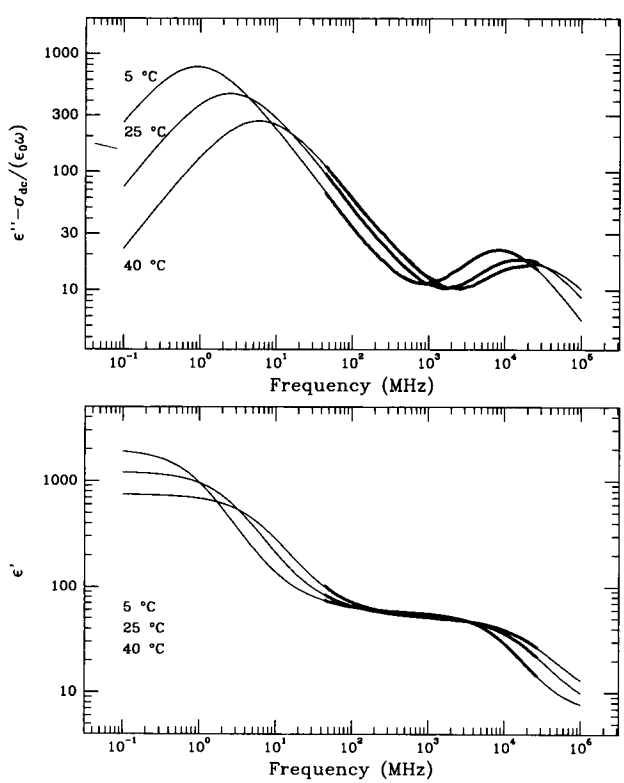

FIGURE 4 Comparison of the dielectric dispersions (β and γ) between Eq. 1 (*thin lines*) and experimental data (*thick lines*) for three different temperatures over an extended frequency range that covers both β- and γ-dispersions entirely.

units experience different dynamic environments such that the distribution of time constants is mainly a reflection of the distributions of the structure and dynamics, which are intrinsic to disordered systems. For our cell suspension system, because local environmental variations at the inhomogeneously charged surfaces of individual cells and on the side chains of proteins give a different local electrostatic field, counterions, which are responsible for the β-dispersion, and bound water layers from the surrounding electrolyte react differently to the external electrical field. These differences can be highly nonlinear, and can be represented mathematically by a distribution around their mean value, which usually results in some form of power-law variation in the dispersion function, regardless of their underlying physical nature.

The parameters of Eq. 4 are determined by means of a complex nonlinear least squares (CNLS) fit, which fits the real and imaginary parts simultaneously and ensures a global fit. The objective function (S) is defined as

$$S(\vec{P}) = \sum_{k=1}^{n} \{W_r(\omega_k)[\epsilon^r_{cc}(\omega_k, \vec{P}) - \epsilon^r(\omega_k)]^2 + W_i(\omega_k)[\epsilon^i_{cc}(\omega_k, \vec{P}) - \epsilon^i(\omega_k)]^2\}, \quad (5)$$

where n is the number of data points, subscript and superscript r and i denote the real and imaginary parts, respectively, and W is the weighting factor. $\vec{P} = \{\epsilon_h, \Delta\epsilon_m, \tau_m, \alpha_m, \sigma; m = 1, 2\}$ represents a set of real parameters. The best-fit values of these parameters are evaluated by minimizing S using the Levenberg-Marquardt algorithm (Press et al., 1988). The fits are remarkably good. Fig. 3 shows the comparison between the CNLS fits and the experimental data at three different temperatures (5, 25, and 40°C). Fig. 4 shows the double Cole-Cole function in an extended frequency range (100 kHz to 100 GHz) to present an overall picture of the dielectric dispersion in the entire radio and microwave fre-

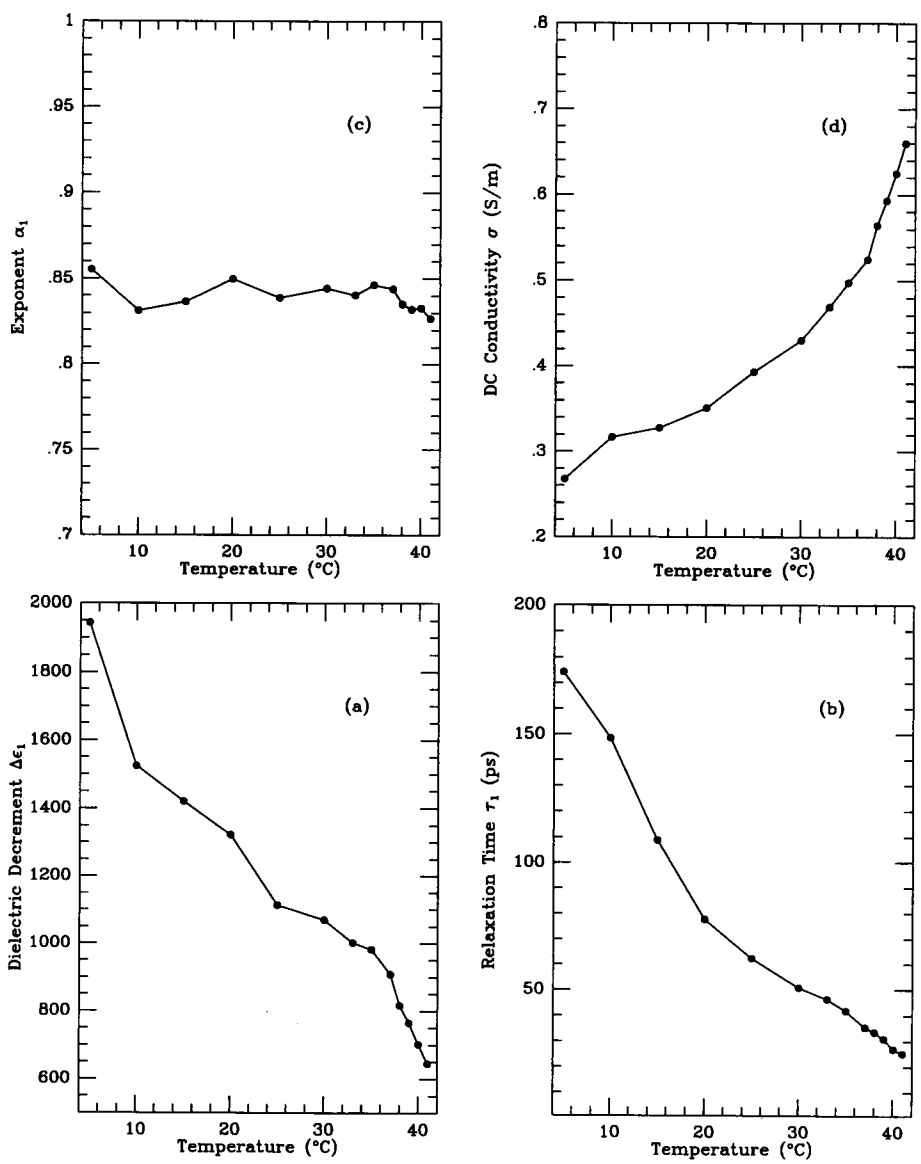

FIGURE 5 Temperature dependence of the parameters of the Cole-Cole function for the β-dispersion ($\Delta\epsilon_1$, τ_1, α_1) and the dc conductivity (σ_{dc}), which are mainly determined by the low-frequency part of the data. The frequency range of the spectra yielding the above parameters is from 45 MHz to 26.5 GHz. Since only the high-frequency tail of the β-dispersion is covered in this frequency range, the above parameters are not well determined.

quency range. Although the absolute values beyond the experimental data may be subject to errors to some extent, these curves are consistent with our current understanding of the dielectric dispersion of cell suspensions.

Fig. 5 shows the temperature dependence for the parameters of the β-dispersion ($\Delta\epsilon_1$, τ_1, α_1) and σ_{dc}, which are mainly determined by the low-frequency portion of the spectra. Since only the high-frequency tail of the β-dispersion is covered in this range, the corresponding parameters are not well determined, especially at low temperatures, so they are only suggestive. However, more and more of the β-dispersion moves into this range when temperature increases so that the accuracy of these parameters becomes better. We wish to stress, however, that the repeatability and accuracy of our dielectric measurements is very good. The only significant error analysis amounts to a χ^2 goodness-of-fit analysis of whether the data fits a particular dispersion. We choose to fit our data with the minimum number of adjustable parameters so that our dispersion parameters are a reliable description of the suspensions. It is actually possible to add other (small) dispersions and obtain apparently even better fits, but the presence of these additional dispersions is highly dubious and we do not include them. The β-dispersion is mainly caused by interfacial polarizations between dissimilar materials. In general, the larger the difference of their dielectric properties, the larger the decrement of the dispersion. When the materials are the same, the dispersion disappears. In our case the dielectric constant of saline is about 80 in the MHz range while the equivalent dielectric constant of cells is about 60. When temperature increases, the dielectric constants of both saline and cells decrease, however, the latter decreases more slowly, which results in a decreasing difference of dielectric constant between cells and saline. Thermally stimulated depolarization can also affect the β-dispersion. At about 35°C, the decrease of the dielectric decrement ($\Delta\epsilon_1$) becomes faster, which may result from an increase of the dielectric constant of the cell membrane induced by a thermally-activated process (Bao et al., 1992).

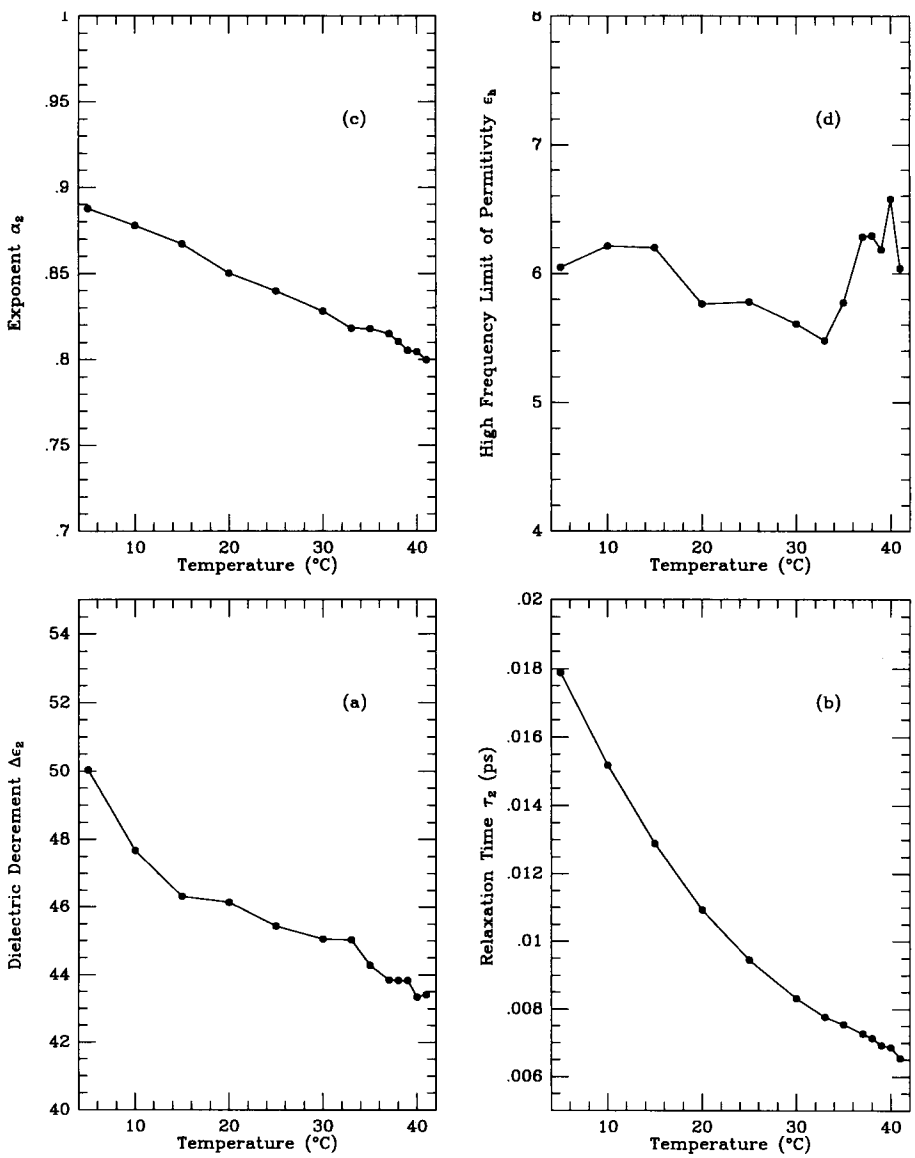

FIGURE 6 Temperature dependence of the parameters of the Cole-Cole function for the γ-dispersion ($\Delta\epsilon_2$, τ_2, α_2) and the high-frequency limit of the dielectric constant (ϵ_h), which are mainly determined by the high-frequency part of the data. The frequency range of the spectra yielding the above parameters is from 45 MHz to 26.5 GHz.

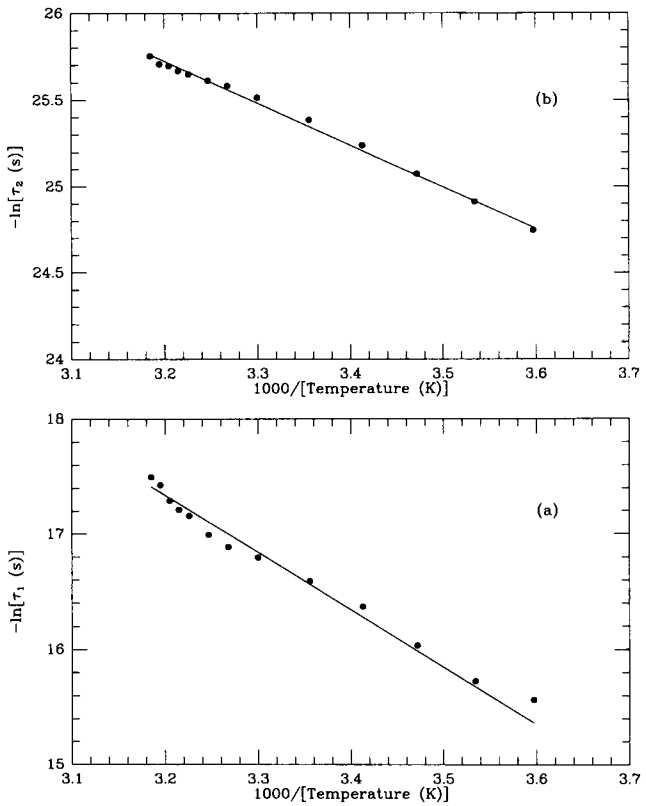

FIGURE 7 Arrhenius plots of the time constants (τ_1 and τ_2) obtained from CNLS fits (●) and their least squares fits (*solid lines*) for β-dispersion (*a*) and γ-dispersion (*b*).

τ_1 decreases with temperature, as shown in Fig. 5 *b*, which may result from an increase in conductivity of the cytoplasm and the extracellular medium. The exponent α_1 in Fig. 5 *c* is almost a constant with temperature, which suggests that the structural and dynamic distributions in and around cell membranes that affect the β-dispersion are more or less temperature-independent. The dc conductivity of the suspension, shown in Fig. 5 *d*, increases with temperature and its rate of increase with temperature becomes higher for temperatures higher than 35°C.

Fig. 6 shows the temperature dependence of the parameters of the γ-dispersion ($\Delta\epsilon_2$, τ_2, α_2) and ϵ_h, which are mainly determined by the high-frequency portion of the spectra. $\Delta\epsilon_2$, shown in Fig. 6 *a*, decreases with temperature, which is consistent with the behavior of water. τ_2 in Fig. 6 *b* decreases with temperature, which results from the increase of the relaxation frequency of water molecules. Fig. 6 *c* shows that α_2 decreases linearly with temperature, suggesting a broader distribution of time constants at higher temperature. The thermal movement of macromolecules will strongly affect the water molecules bound to them, and a higher temperature causes a higher degree of disorder, which gives a broader distribution of time constants. The dielectric background of the γ-dispersion, ϵ_h, shown in Fig. 6 *d*, which is determined by microscopic system structure, varies nonlinearly with temperature.

Measurements made at different temperatures show the dispersion maximum shift in the manner of a thermally activated process, which is usually expressed as an Arrhenius relation

TABLE 1 Parameters from the linear least squares fits of Arrhenius plots

Parameter	τ_∞ (s)	ΔH (kcal/mol)
β-Dispersion	0.036 ± 0.024	9.87 ± 0.42
γ-Dispersion	0.035 ± 0.003	4.80 ± 0.06

Fit and data are shown in Fig. 7.

$$\tau = \tau_\infty e^{\Delta H/RT} \tag{6}$$

where τ_∞ is a prefactor, ΔH is the activation enthalpy, and R is the molar gas constant. τ_∞ and ΔH can be found with an Arrhenius plot, shown in Fig. 7, with a linear least squares fit. The results are given in Table 1.

In conclusion, we have described our measurement technique and calibration method and used them to study the dielectric properties of human erythrocytes. Two major dispersions (β and γ), characterized by two Cole-Cole functions, and a much smaller dispersion between them have been observed in the frequency range from 45 MHz to 26.5 GHz, and over a temperature range from 5 to 40°C. The low-frequency part of both ϵ' and ϵ'' shows a significant jump in the temperature range from 35 to 40°C. At around 1 GHz, ϵ' shows a stronger temperature dependence at lower temperatures. At about 3.4 GHz, ϵ' is almost independent of temperature. The temperature dependence of the time constants suggests that the underlying physical relaxation mechanism is a thermally activated process, and the activation enthalpies for the β- and γ-dispersions are 9.87 ± 0.42 kcal/mol and 4.80 ± 0.06 kcal/mol, respectively.

APPENDIX

For a linear two-port network, we always have

$$\begin{pmatrix} b_1 \\ b_2 \end{pmatrix} = \begin{pmatrix} s_{11} & s_{12} \\ s_{21} & s_{22} \end{pmatrix} \begin{pmatrix} a_1 \\ a_2 \end{pmatrix}, \tag{A1}$$

where s_{ij} $(i, j = 1, 2)$ are the elements of the scattering matrix, a_i and b_i $(i = 1, 2)$ are incident and reflected waves, respectively, and $i = 1$ and 2 corresponds to the port connected to the network analyzer and the port dipped into the sample, respectively. With $\rho_m = b_1/a_1$ and $\Gamma = b_2/a_2$, we get the following equation

$$\Gamma = \frac{\rho_m - s_{11}}{s_{22}\rho_m + s_{12}s_{21} - s_{11}s_{22}}. \tag{A2}$$

With Eqs. 1 and 2, we finally have

$$\rho_m = \frac{A_2 + A_3\epsilon}{A_1 + \epsilon}, \tag{A3}$$

where A_1, A_2, and A_3 are given by

$$A_1 = \frac{1 - s_{22}}{j\omega Z_0 C_0(1 + s_{22})} + \frac{C_f}{C_0}, \tag{A4}$$

$$A_2 = \frac{s_{11} - s_{11}s_{22} + s_{12}s_{21}}{j\omega Z_0 C_0(1 + s_{22})} + \frac{C_f(s_{11} + s_{11}s_{22} - s_{12}s_{21})}{C_0(1 + s_{22})}, \tag{A5}$$

$$A_3 = \frac{s_{11} + s_{11}s_{22} - s_{12}s_{21}}{1 + s_{22}}. \tag{A6}$$

Since Z_0, C_f, and C_0 have be combined into A_1 and A_2, individual estimation

of the lumped circuit parameters becomes unnecessary. Although Eq. A.3 has been reported previously (Wei and Sridhar, 1989), we have derived it in a different way. The advantage of our derivation is that Z_0, C_o, and C_f are explicitly shown in A_1 and A_2. Substituting "short" ($\Gamma = -1$ and $\rho_m = \rho_m^s$) into Eq. A.3, we have

$$A_3 = \rho_m^s, \tag{A7}$$

where superscript s represents short. Substituting "open" ($\epsilon = 1$ and $\rho_m = \rho_m^o$) and "standard liquid" ($\epsilon = \epsilon_s$ and $\rho_m = \rho_m^l$) into Eq. 9, we have

$$\rho_m^o A_1 - A_2 - A_3 = -\rho_m^o, \tag{A8}$$

$$\rho_m^l A_1 - A_2 - \epsilon_s A_3 = \epsilon_s \rho_m^l, \tag{A9}$$

where superscripts o and l stand for open and standard liquid, respectively, and ϵ_s is the dielectric constant of saline. Solving the above complex equations gives A_1, A_2, and A_3. After obtaining these three complex constants, the unknown complex dielectric constant can be found with Eq. 3 from ρ_m at each frequency point. Although only the coaxial line and SMA connector are taken into account by the scattering matrix in the above derivation, we find that other artifacts, such as the effects of the sample container, can be eliminated quite well. It is interesting to notice that Eq. 3 has the same mathematical form as Eq. 16 in Bao et al. (1993), despite the fact that the latter was derived using a completely different approach.

We thank Dr. Kee W. Rhee, Chang-Shuoh Lee, and Douglas Wiley for some preliminary work on the measurement system, Dr. Ewa Czerska for help in obtaining erythrocytes, and Li Li for help in preparing samples.
This work was supported by Office of Naval Research contracts N00014-84K-0550 and N00014-92-J-1831.

REFERENCES

Asami, K., Y. Takahashi, and S. Takashima. 1988. Dielectric properties of mouse lymphocytes and erythrocytes. *Biochim. Biophys. Acta.* 1010: 49–55.

Athey, T. W., M. A. Stuchly, and S. S. Stuchly. 1982. Measurement of radio frequency permittivity of biological tissues with an open-ended coaxial line: part I. *IEEE Trans. Microwave Theory Technique.* 30:82–86.

Baker-Jarvis, J., E. J. Vanzura, and W. A. Kissick. 1990. Improved technique for determining complex permittivity with the transmission/reflection method. *IEEE Trans. Microwave Theory Technique.* 38:1096–1103.

Ballario, C., A. Bonincontro, and C. Cametti. 1984. Conductivity of normal and pathological human erythrocytes (homozygous β-thalassemia) at radiowave frequencies. *Eur. Biophys. J.* 12:161–166.

Bao, J.-Z., C. C. Davis, and R. E. Schmukler. 1992. Frequency domain impedance measurements of erythrocytes: constant phase angle impedance characteristics and a phase transition. *Biophys. J.* 61: 1427–1434.

Bao, J.-Z., C. C. Davis, and R. E. Schmukler. 1993. Impedance spectroscopy of human erythrocytes: system calibration and nonlinear modeling. *IEEE Trans. Biomed. Eng.* 40:364–378.

Bone, S., B. Z. Ginzburg, G. Wilson, and B. Zaba. 1993. Time-domain dielectric spectroscopy applied to cell suspensions. *Phys. Med. Biol.* 38: 511–520.

Bottcher, C. J. F., and P. Bordewijk. 1978. Theory of Electric Polarization, 2nd ed., Vol. 2. Elsevier, New York.

Chou, C.-K. 1992. Evaluation of microwave hyperthermia applicators. *Bioelectromagnetics.* 13:581–597.

Colpitts, B. G. 1993. Temperature sensitivity of coaxial probe complex permittivity measurements: experimental approach. *IEEE Trans. Microwave Theory Techniques.* 41:229–233.

Dissado, L. A. 1990. A fractal interpretation of the dielectric response of animal tissues. *Phys. Med. Biol.* 35:1487–1503.

Dube, D. C. 1988. Dielectric measurements on substrate materials at microwave frequencies using a cavity perturbation technique. *J. Appl. Phys.* 63:2466–2468.

Edwards, G., G. Ying, and J. Tribble. 1992. Role of counterions in the gigahertz relaxation of wet DNA. *Phys. Rev. A.* 45:8344–8347.

Foster, K. R., and E. A. Cheever. 1992. Microwave radiometry in biomedicin—a reappraisal. *Bioelectromagnetics.* 13:567–579.

Grochulski, T., L. Pszczolkowski, and M. Kempka. 1992. Applicability of extended hydrodynamical model to dielectric relaxation in simple polar liquids. *Phys. Rev. Lett.* 68:3635–3637.

Macdonald, J. R. 1987. Measurement technique and data analysis. *In* Impedance Spectroscopy. J. R. Macdonald, editor. John Wiley and Sons, New York. 173–188.

Malmberg, C. G., and A. A. Maryott. 1956. Dielectric constant of water from 0° to 100°C. *J. Res. Natl. Bureau Standards.* 56:1–8.

Michaelson, S. M., and J. C. Lin. 1987. Biological Effects and Health Implications of Radiofrequency Radiation. Plenum Press, New York.

Nee, T.-W., and R. W. Zwanzig. 1970. Theory of dielectric relaxation in polar liquids. *J. Chem. Phys.* 52:6353–6363.

Ngai, K. L. 1987. Evidences for universal behavior of condensed matter at low frequencies/long times. *In* Non-Debye Relaxation in Condensed Matter. T. V. Ramakrishnan and M. R. Lakshmi, editors. World Scientific, New Jersey.

Niklasson, G. A. 1987. Fractal aspects of dielectric response of charge carriers in disordered materials. *J. Appl. Phys.* 62:R1-R14.

Pethig, R. 1984. Dielectric properties of biological materials: biophysical and medical application. *IEEE Trans. Electrical Insulation.* 5:453–474.

Press, W. H., B. P. Flannery, S. A. Teukolsky, and W. T. Vetterling. 1988. Numerical Recipes in C. Cambridge University Press, Cambridge, UK.

Schroeder, M. 1991. Fractals, Chaos, Power Laws. W. H. Freeman and Company, New York.

Schwan, H. P. 1957. Electrical properties of tissue and cell suspension. *In* Advances in Biological and Medical Physics. J. H. Lawrence and C. A. Tobia, editors. Academic Press, New York. 147–209.

Schwan, H. P. 1985. Dielectric properties of cells and tissues. *In* Interactions between Electromagnetic Field and Cells. A. Chiabrera, C. Nicolini, and H. P. Schwan, editors. Plenum Publishing Corp., New York. 75–98.

Schwan, H. P., and K. R. Foster. 1980. RF-field interactions with biological systems: electrical properties and biophysical mechanisms. *Proc. IEEE.* 68:104–113.

Steinhoff, H.-J., B. Kramm, G. Hess, C. Owerdieck, and A. Redhardt. 1993. Rotational and translational water diffusion in the hemoglobin hydration shell: dielectric and proton nuclear relaxation measurements. *Biophys. J.* 65:1486–1495.

Stogryn, A. 1971. Equation for calculating the dielectric constant of saline solution. *IEEE Trans. Microwave Theory Techniques.* 19:733–736.

Stuchly, M. A., M. M. Brady, S. S. Stuchly, and G. Gajda. 1982. Equivalent circuit of an open-ended coaxial line in a lossy dielectric. *IEEE Trans. Instr. Measurement.* 31:116–119.

Wei, Y.-Z., and S. Sridhar. 1989. Technique for measuring the frequency-dependent complex dielectric constants of liquids up to 20 GHz. *Rev. Sci. Instr.* 60:3041–3046.

Weyl, P. K. 1964. On the change in electrical conductance of seawater with temperature. *Limnol. Oceanogr.* 9:75–78.

Zhou, H.-X., and B. Bagchi. 1992. Dielectric and orientational relaxation in a Brownian dipolar lattice. *J. Chem. Phys.* 97:3611–3620.